Pure Appl. Chem., Vol. 73, No. 12, pp. 1979–1991, 2001.

Direct electrochemistry of redox proteins or enzymes at various film electrodes and their possible applications in monitoring some pollutants*

Naifei Hu

Department of Chemistry, Beijing Normal University, Beijing 100875, China

Abstract: Water-insoluble films modified on the surface of solid electrodes may provide a unique microenvironment for electron transfer of some redox proteins or enzymes. The film materials can be two-tail surfactants, or composites of polyion-surfactant or clay-surfactant. Both surfactant and composite films cast on surface of electrodes are self-assembled into an ordered multibilayer structure, which is very similar to the bilayer structure of biological membrane. Amphiphilic polymers can also be used for making films. Incorporated heme proteins such as myoglobin (Mb), hemoglobin (Hb), or horseradish peroxidase (HRP) in these films demonstrated reversible voltammetry. Studies of direct electrochemistry of these proteins in various films by our group are reviewed in this paper. The protein films may provide a good model for study of electron transfer process in biological systems. The electrocatalytic properties of the protein films may also be applied to monitor some pollutant substrates.

INTRODUCTION

Direct electrochemistry of redox proteins or enzymes attracts increasing interest nowadays because study of direct electron transfer between proteins and electrodes can provide a model for the mechanism study of electron exchange among proteins or enzymes in biological system, and establish a foundation for fabricating new kinds of biosensors, catalytic bioreactors, and biomedical devices without using chemical mediators [1,2].

However, it is usually difficult for redox proteins in solution to transfer electron directly with bare electrodes. There are several possible reasons for this. Unfavorable orientation of protein molecules on electrode surface may hinder the electron exchange between the electrode and the electroactive center of proteins, which is usually deeply buried inside the polypeptide chains. The "bad" orientation may also increase the distance between the redox center and electrodes, and thus increase the difficulty of direct electrochemistry of the proteins. The adsorption of macromolecular impurities or denatured proteins on electrode surface may also block the electron exchange between proteins and electrodes [3,4].

Some researchers used a mediator as a bridge between proteins in solution and electrodes. The mediator is usually a small molecular compound that is electroactive itself. The mediator can efficiently transport electrons with proteins and electrodes, respectively, and thus shuttle electrons between them. However, this indirect electrochemistry of proteins complicates the electrode process of proteins.

Some researchers make use of a promoter to facilitate direct electrochemistry of proteins [4]. The promoter is also a small molecular compound, but it is electroinactive. The adsorption of promoter on electrode surface may be helpful for proteins to take its favorable orientation toward electrodes and decrease the distance between the redox center and electrodes, and then enhance the electron transfer

*An issue of reviews and research papers based on presentations made at the IUPAC/ICSU Workshop on Electrochemistry and Interfacial Chemistry in Environmental Clean-up and Green Chemical Processes, Coimbra, Portugal, 6–7 April, 2001.

between them. For example, Hill *et al*. first reported quasi-reversible voltammetry of cytochrome c at Au electrodes with a promoter of 4,4′-bipyridyl in solution [5]. Proteins in the promoter system are in solution phase.

A relatively new avenue to realize direct electrochemistry of proteins is to incorporate proteins into films that are modified on electrode surface [2,6]. Thin films may provide a well-defined microenvironment for proteins and enhance electron transfer between proteins and electrodes. For instance, Rusling and coworkers have developed procedures for preparing surfactant films into which proteins are incorporated [6]. Myoglobin (Mb) embedded in didodecyldimethylammonium bromide (DDAB) films cast on pyrolytic graphite (PG) electrodes gave quite reversible cyclic voltammogram [7]. Mb was believed to display only very slow electron transfer at bare or "naked" electrodes. Armstrong *et al*. studied "protein film voltammetry" with a variety of different configurations [8]. Bianco *et al*. found that c-type cytochromes in lipid or polymer films gave reversible voltammograms [9,10]. Direct electrochemistry of cytochrome P450 [11] and hydrogen peroxidase (HRP) [12] at film electrodes were also reported. Since the incorporated protein is always in the film phase, the amount of protein used is much smaller than that in solution phase. This very limited amount of protein sometimes is crucial, especially for the study of some expensive enzymes. The protein films may also establish a new method for immobilization of proteins on electrode surface, which may be applied more easily to fabricating the corresponding biosensor.

In recent years, our group has studied various film systems in which embedded proteins demonstrated direct and reversible voltammetry at underlying PG electrodes. These protein films showed good stability in blank buffers and were amenable to a variety of electrochemical, spectroscopic and other experiments. In this paper, the properties of the protein films are reviewed briefly. Electrochemical catalysis of some environmental pollutants at the protein film electrodes was also studied. Our research mainly focused on some heme proteins or enzymes, such as myoglobin (Mb), hemoglobin (Hb), and horseradish peroxidase (HRP). All these proteins have relatively small molecular size compared with most proteins, and have the same heme prosthetic group, which is usually electroactive and the redox center of the protein. All potentials reported in this overview are vs SCE.

VARIOUS TYPES OF FILMS

Our group studied different types of protein films, and some of the film materials are briefly introduced here.

Surfactant films

Typical surfactants we used to make films include didodecyldimethylammonium bromide (DDAB), dihexadecylphosphate (DHP), and dimyristoyl phosphatidylcholine (DMPC) (Fig. 1). They are all

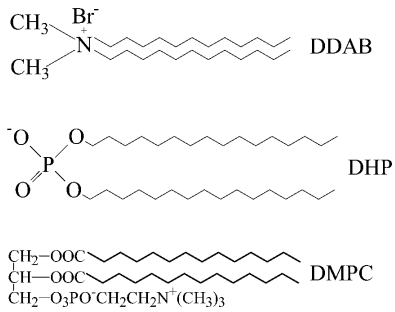

Fig. 1 Chemical structure of DDAB, DHP, and DMPC.

water-insoluble and have relatively long double chains. DMPC is a lipid component, while DDAB and DHP are synthesized, but are also biomembrane-like surfactants. DDAB is positively charged, DHP is negatively charged, while DMPC has a zwitterionic head group. When the aqueous surfactant dispersion is cast onto surface of solid substrates such as PG electrodes, after the solvent is evaporated, the surfactant can be self-assembled into a multibilayer structure. Thus, the films would provide a biomembrane-like microenvironment for incorporated proteins.

Polyion-surfactant or clay-surfactant composite films

With electrostatic attraction between polyion (or clay) and oppositely charged surfactant, the polyion (or clay) and surfactant can form neutral, water-insoluble complex composite. These polyion-surfactant or clay-surfactant composite films have a multibilayer structure and fundamental characteristics similar to surfactant films alone, and may have better stability than the latter owing to introduction of polymer or clay backbones in the films. Thus, the films would also provide a biomembrane-like microenvironment for incorporated proteins. Some examples of polyions we used are polystyrenesulfonate (PSS), polyacrylic acid (PAA), polyvinyl sulfate (PVS), and poly(diallyldimethylammonium) (PDDA) (Fig. 2).

The conceptual pictures of protein-surfactant and protein-surfactant-clay composite films are demonstrated in Fig. 3.

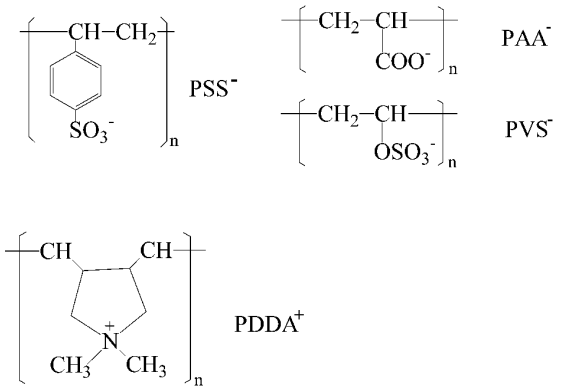

Fig. 2 Chemical structure of PSS, PAA, PVS, and PDDA.

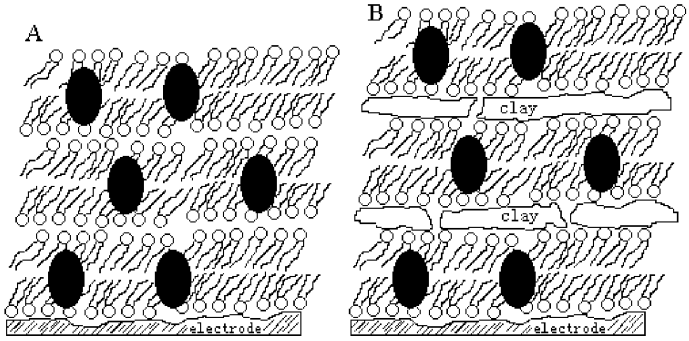

Fig. 3 Conceptual picture of (A) protein-surfactant and (B) protein-surfactant-clay composite films.

Amphiphilic polymer films

The amphiphilic polymers we used to make films include poly(ester sulfonic acid) or Eastman AQ and polyacrylamide (PAM) (Fig. 4). These polymers have hydrophobic backbone and hydrophilic groups, and can be considered as polymeric surfactants. The films can absorb a large amount of water from aqueous solution and form hydrogel, but they are water-insoluble and very stable in aqueous solution. The hydrogel films can provide a favorable microenvironment for incorporated proteins.

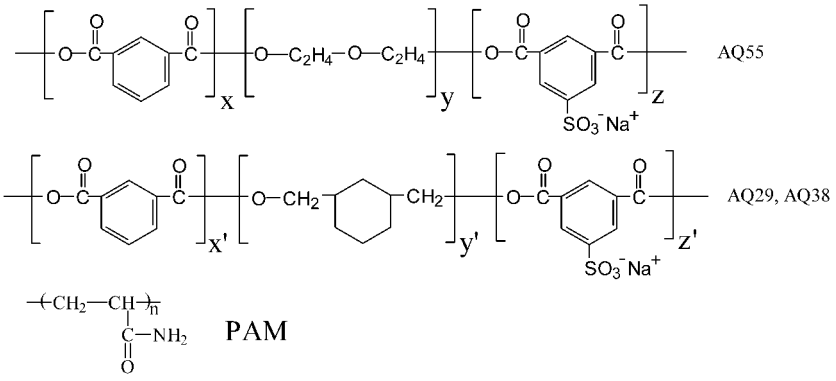

Fig. 4 Chemical structure of AQ and PAM.

DIRECT ELECTROCHEMISTRY OF PROTEINS IN FILMS

Cyclic voltammetry (CV)

The heme proteins in the above three kinds of films showed good direct electrochemistry. For example [13], when Hb-DMPC films cast on PG electrodes were placed in pH 5.5 buffers containing no Hb, a pair of well-defined and quite reversible CV peaks at –0.3 V vs SCE appeared, characteristic of Hb heme Fe(III)/Fe(II) redox couple (Fig. 5). DMPC films without Hb showed no CV signal at all in this potential window. The bare PG electrodes in Hb solution gave a very small CV signal. Thus, the electron transfer between Hb and PG electrodes was greatly enhanced in a DMPC film environment.

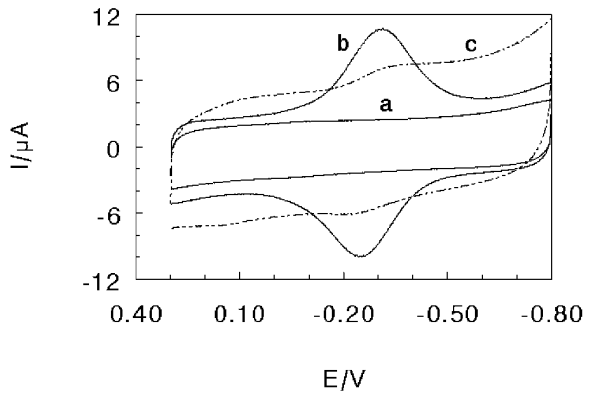

Fig. 5 Cyclic voltammograms at 0.5 V s^{-1} in pH 5.5 buffers for (a) DMPC and (b) Hb-DMPC films, and (c) bare PG in 1.7×10^{-4} M Hb solutions. Adapted from ref. 13 with permission.

Another example is Mb-DDAB-PAA composite films (Fig. 6) [14]. Steady-state CVs for Mb-DDAB-PAA films in pH 5.5 buffers showed two pairs of near-reversible reduction–oxidation peaks. The first pair centered at about –0.2 V was attributed to Mb Fe(III)/Fe(II) redox couple, while the second one centered at about –1.1 V was considered to be attributed to Mb Fe(II)/Fe(I) redox couple.

The first redox peak pair of all the protein films studied here had an approximately symmetric peak shape and nearly equal heights of reduction and oxidation peaks. The reduction peak currents increased linearly with scan rates. Integration of reduction peaks at different scan rates gave nearly constant charge values. All these are characteristic of diffuseless, thin-layer electrochemical behavior [15], suggesting that all electroactive heme Fe(III) in the films is converted to heme Fe(II) on the forward cathodic scan, with full conversion of heme Fe(II) back to heme Fe(III) on the reverse anodic scan.

The stability of the protein films was tested by CV with two different methods. In the solution studies, the protein film electrodes were stored in buffers all the time, and CVs were performed periodically. Alternatively, the film electrodes were dried in air for most of the storing time, and CVs were run periodically after returning the dry films to buffers. With these two methods, most of the protein films showed excellent stability. Usually, they were stable for several weeks. For some films, especially for the composite films and hydrogel polymer films, they were stable for even a few months.

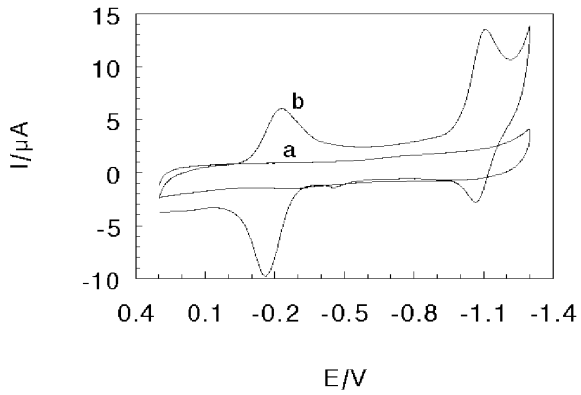

Fig. 6 Cyclic voltammograms at 0.1 V s^{-1} in pH 5.5 buffers for (a) DDAB-PAA and (b) Mb-DDAB-PAA films. Adapted from ref. 14 with permission.

Influence of pH on voltammetry

The pH of external solution had great influence on the CV of protein films. For instance, an increase in buffer pH caused a negative shift in potential for both reduction and oxidation CV peaks for Hb-DDAB-clay composite films [16]. The formal potential ($E^{\circ\prime}$), estimated as the midpoint of reduction and oxidation peak potentials, varied linearly with pH from 4.5 to 11 with a slope of –52 mV pH^{-1} (Fig. 7). This value is reasonably close to the theoretical value of –59 mV pH^{-1} at 25 °C [17], indicating that a single proton transfer is coupled to a reversible electron transfer for each heme group of Hb. Different protein films have different linear ranges and different slopes in their $E^{\circ\prime}$-pH plot, but the electron transfer of protein heme Fe(III)/Fe(II) couple is always accompanied by proton transportation in all the films.

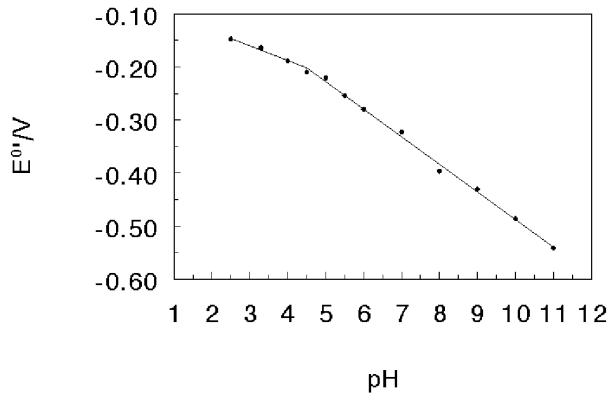

Fig. 7 Influence of pH on formal potential for Hb-DDAB-clay films from CV at 0.1 V s^{-1}. Adapted from ref. 16 with permission.

Estimation of k_s and $E^{\circ\prime}$ by square wave voltammetry

Square wave voltammetry (SWV) has better signal-to-noise ratio and resolution than CV [18] and thus was used here to estimate the apparent heterogeneous electron transfer rate constant (k_s) and formal potential ($E^{\circ\prime}$) for the heme Fe(III)/Fe(II) couple of proteins. The procedure employed nonlinear regression analysis for SWV forward and reverse curves, with the combination of the thin-layer SWV model [19] and the formal potential dispersion model, which was discussed in detail previously [20,21]. The results for different protein films are presented in Table 1.

Table 1 Apparent heterogeneous electron-transfer rate constants and formal potentials for protein films on PG electrodes in pH 7.0 buffers containing no protein.

Films	Average k_s/s^{-1}	Average $E^{\circ\prime}$ vs. SCE/V		Reference
		CV	SWV	
Mb-DDAB	31 ± 3	–0.228	–0.240	21
Mb-DMPC	59 ± 9	–0.326	–0.342	21
Mb-DLPC	50 ± 8	–0.329	–0.343	21
Mb-DDAB-PAA	11 ± 1	–0.231	–0.212	14
Mb-DDAB-PVS	58 ± 7	–0.196	–0.202	22
Mb-DDAB-PSS	28 ± 5	–0.236	–0.255	23
Mb-DHP-PDDA	27 ± 3	–0.323	–0.326	24
Mb-DDAB-clay	44 ± 8	–0.252	–0.243	25
Mb-AQ	52 ± 6	–0.362	–0.340	26
Hb-DMPC	70 ± 9	–0.329	–0.331	13
Hb-DDAB-PSS	33 ± 5	–0.220	–0.204	27
Hb-DDAB-clay	75 ± 8	–0.309	–0.308	16
Hb-AQ	62 ± 7	–0.341	–0.324	28
Hb-PAM	45 ± 8	–0.320	–0.312	29
HRP-AQ	42 ± 4	–0.360	–0.314	30

The k_s values for different protein films are different, but all of them in the same magnitude. Relatively high k_s values indicate that these films provide a favorable microenvironment for these proteins, and greatly enhance the rate of electron transfer between the proteins and electrodes compared

with the proteins in solution at bare PG electrodes. The $E^{\circ\prime}$ values for the same protein in different films are different. This confirms a specific influence of the film environment on formal potential for heme proteins. Film components may change potentials by interaction with the protein or by their influence on the electrode double layer [21].

CHARACTERIZATION OF PROTEIN FILMS

UV-vis and reflectance absorption infrared spectroscopy

The positions of the Soret absorption band of heme can provide information about the possible denaturation of heme proteins [31]. Thus, UV–vis spectroscopy was used here to observe the change of Soret band for the protein films. For example, both dry films cast from Hb and Hb-PAM on transparent indium tin oxide (ITO) slides showed Soret bands at 415 nm (Fig. 8) [29], suggesting that Hb in dry PAM films has a secondary structure nearly the same as the native state of Hb in dry Hb films alone. The position of the Soret band depended on pH when Hb-PAM films were placed into buffer solutions. At pH between 4.5 and 11.0, the Soret band appeared at 405 nm, same as that of Hb in buffer solutions at medium pH. PAM hydrogel films provide a basically aqueous environment for Hb. Thus, it is reasonable that Hb in PAM films showed the same Soret band position as in water solution. When pH was changed toward more acidic or more basic direction, the Soret band showed significant blue shift. This indicates Hb in PAM films might denature to considerable extent in this relatively extreme pH environment.

The shape and position of infrared bands of Amide I (1600–1700 cm^{-1}) and Amide II (1500–1600 cm^{-1}) can provide detailed information on the secondary structure of polypeptide chain of proteins [32], and reflectance absorption infrared (RAIR) spectroscopy was used here to detect conformational change of HRP in AQ films (Fig. 9) [30]. The HRP films alone showed IR amide I band at 1643 cm^{-1} and amide II band at 1537 cm^{-1}. For HRP-AQ films, the bands of amide I and amide II showed the

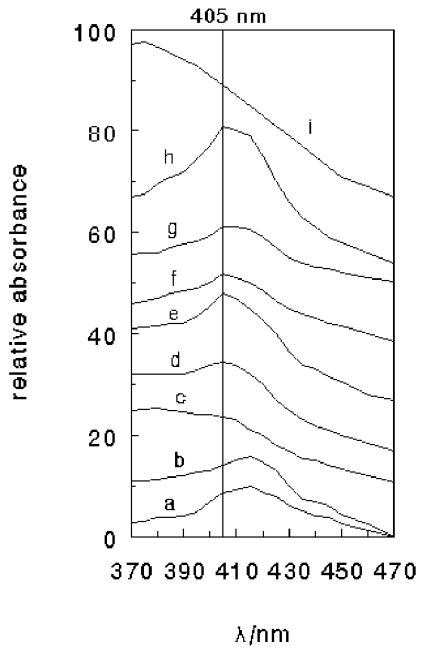

Fig. 8 UV–vis spectra of Hb and Hb-PAM films on ITO slides: (a) Hb dry film, (b) Hb-PAM dry film; Hb-PAM films in different pH buffer solutions: (c) pH 4.0, (d) pH 4.5, (e) pH 5.5, (f) pH 7.0, (g) pH 10.0, (h) pH 11.0, (i) pH 12.0. Adapted from ref. 29 with permission.

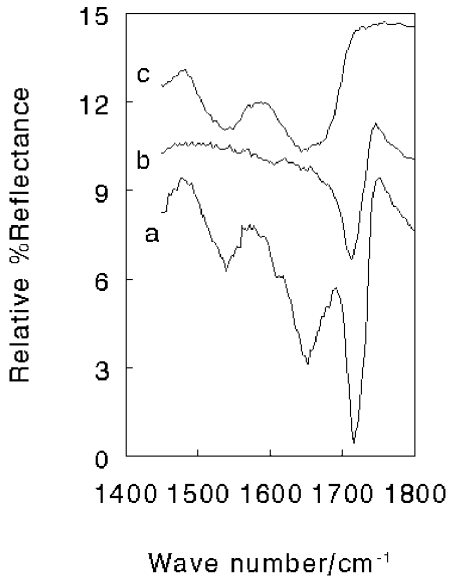

Fig. 9 Reflectance absorption infrared spectra of (a) HRP-AQ, (b) AQ, and (c) HRP films. Adapted from ref. 30 with permission.

shapes and positions very similar to those of the HRP film alone, indicating that HRP in AQ films essentially retained its native secondary structure. A large IR band at 1716 cm^{-1} was observed for HRP-AQ films, but not seen for HRP films alone. This band should be assigned to AQ, since AQ films alone showed a single infrared band at this position in the tested range.

The results of UV–vis and RAIR spectroscopy demonstrate that in general, the proteins keep the secondary structure similar to their native state in the studied films at the medium pH.

X-ray diffraction (XRD) and differential scanning calorimetry (DSC)

The small angle XRD for polyion-surfactant or clay-surfactant composite films can be used to obtain the inter-layer basal spacing of the films. Take DHP-PDDA films as an example (Fig. 10) [24]. A main

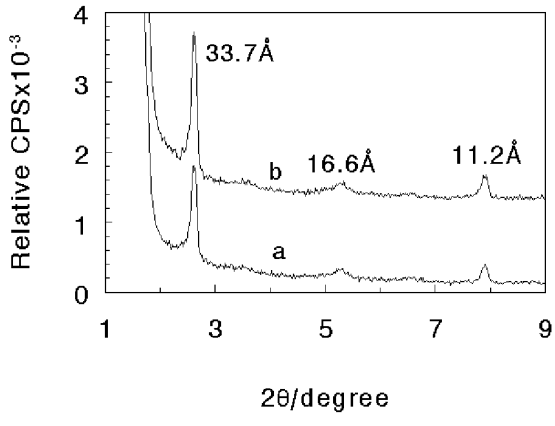

Fig. 10 X-ray diffraction of (a) DHP-PDDA and (b) Mb-DHP-PDDA films. Adapted from ref. 24 with permission.

XRD peak gave PDDA basal spacing of 33.7 Å, while two other much smaller peaks gave about 1/2 and 1/3 Bragg's spacing compared to the main peak, which were identified as the second- and third-order diffraction, respectively. Similar patterns and almost the same peak positions were observed in XRD experiments for Mb-DHP-PDDA films, indicating that incorporation of Mb essentially did not enlarge the interlayer spacing of DHP-PDDA films. Rather sharp XRD main peaks suggest well-defined layer orders in both films.

DSC may provide information on phase transition of lipid bilayers [33] and was used here to confirm the formation of bilayer structure of surfactant. DHP-PDDA films showed transition temperature at 72.6 °C (Table 2) [24], very close to 72 °C for DHP films alone, indicating the films undergo transition from solid-like gel phase to more fluid liquid-crystal phase at this temperature, and DHP in the composite films is arranged in a tail-to-tail bilayer structure. Mb-DHP-PDDA films showed two DSC peaks at 69.7 and 74.0 °C. The first one was very close to the melting point of pure Mb at 69.0 °C, and should be assigned to melting of Mb in the films. Thus, the second DSC peak of the films at 74.0 °C is most probably attributed to the phase transition of DHP lipid in the films, showing that DHP-PDDA films essentially maintain the multibilayer structure after incorporation of Mb.

Results of XRD and DSC for DHP-PDDA films support the proposal that surfactant DHP is self-assembled into an ordered bilayer structure that is complexed with and sandwiched by PDDA backbone layers, and thousands of such bilayer were parallel stacked in the films. Other polyion-surfactant or clay-surfactant films showed similar structure features.

Table 2 Gel-to-liquid crystal phase transition temperatures measured by DSC for films of lipids and Mb-lipids

Films	T_c/°C		Reference
DHP		72	34
Mb-DHP		72	34
DHP-PDDA		72.6	24
Mb-DHP-PDDA	69.7	74.0	24
Mb	69.0		24

ELECTROCATALYTIC REDUCTION OF ORGANOHALIDES WITH PROTEIN FILMS

Organohalides are important environmental pollutants arising from various sources, such as solvents and pesticides. Thus, it is significant to establish good methods to monitor or destroy these pollutants. Protein films showed very nice catalytic properties, and can be employed as the foundation of fabricating biosensors or bioreactors to determine or destroy organohalides.

The electrocatalytic reduction of trichloroacetic acid (TCA) by Hb-PAM films was tested by CV [29]. When TCA was added to a pH 5.5 buffer, an increase in the HbFe(III) reduction peak at about –0.3 V for Hb-PAM films was observed (Fig. 11). This was accompanied by a disappearance of the HbFe(II) oxidation peak. The reduction peak current for HbFe(III) increased with the concentration of TCA in the solution. These results indicate reaction of HbFe(II) with TCA in a catalytic cycle. For comparison, the direct reduction of TCA on PAM films with no Hb incorporated would appear at the potential of more negative than –0.8 V. Thus, Hb-PAM films lowered the reduction overpotential of TCA by at least 0.5 V. The catalytic efficiency, expressed as the ratio of HbFe(III) reduction peak current in the presence (I_c) and absence of TCA (I_d), I_c/I_d, decreased with increase of scan rate, also characteristic of electrochemical catalysis [35].

The electrocatalytic reduction of benzene hexachloride (BHC) by Mb-DDAB-PSS films was also observed by CV [23]. The results showed that the catalytic reduction peak of BHC was not observed at the potential of the first reduction peak, but at that of the second one for Mb-DDAB-PSS films. When

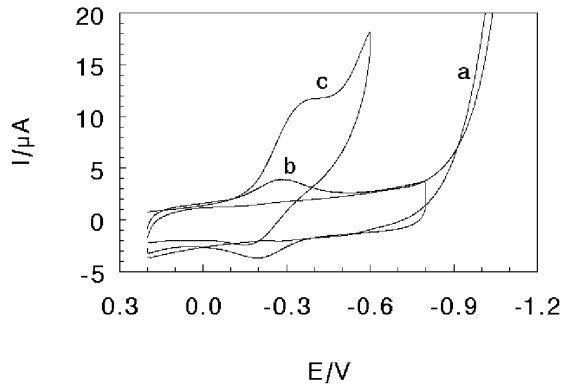

Fig. 11 Cyclic voltammograms at 0.1 V s^{-1} in pH 5.5 buffer solutions for (a) PAM film with 0.07 M TCA present in solution, (b) Hb-PAM film with no TCA present, and (c) Hb-PAM film with 0.07 M TCA present in solution. Adapted from ref. 29 with permission.

BHC was added into a pH 5.5 buffer solution, an increase in the MbFe(II) reduction peak at –1.1 V was observed (Fig. 12). This increase in reduction peak for MbFe(II) was accompanied by the disappearance of the MbFe(I) oxidation peak. The reduction peak current for MbFe(II) increased with the concentration of BHC in the solution. These results indicate reaction of MbFe(I) with BHC in a catalytic cycle. For DDAB-PSS films with no Mb incorporated, the direct reduction peak of BHC would appear at the potential of more negative than –1.5 V.

The electrochemical catalysis of reduction of perchloroethylene (PCE) by Mb-DDAB-PAA films was also demonstrated by CV and used to detect and determine PCE in solution [14]. The reduction peak height of PCE on Mb-DDAB-PAA films had a linear relationship with PCE concentration in the range of 10–100 μM with correlation coefficient of 0.999 and detection limit of 2 μM. The level-off of the peak currents was observed when the concentration of PCE was above 100 μM. The electrocatalysis of other organohalides with Mb-DDAB-PAA films was also studied [14]. For instance, trichloroethylene (TCE) showed electrocatalytic behaviors similar to PCE. However, trichloroacetic acid (TCA) did not show any catalytic behavior at the Mb-DDAB-PAA films at all, indicating the films have some selectivity to the substrates. Results of linear range of calibration curve and detection limit for deter-

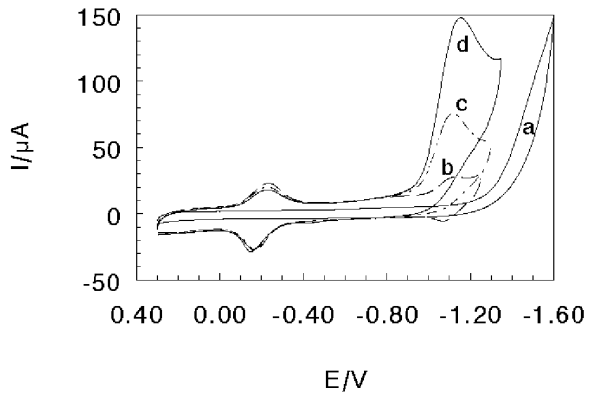

Fig. 12 Cyclic voltammograms at 0.5 V s^{-1} in pH 5.5 buffer solutions for (a) DDAB-PSS film with 10 μM BHC present, (b) Mb-DDAB-PSS film with no BHC present, (c) Mb-DDAB-PSS film with 10 μM BHC, and (d) Mb-DDAB-PSS film with 17 μM BHC. Adapted from ref. 23 with permission.

mination of some organohalides with protein film electrodes are presented in Table 3. These results suggest the potential application of the stable protein films as a sensor for detecting some organohalide pollutants.

Table 3 Linear range of calibration curve and detection limit for determination of some organohalides with protein film electrodes

Films	Substrates	Linear range/μM	Detection limit/μM	Correlation coefficient	Reference
Mb-DDAB-PAA	PCE	10–100	2	0.999	14
Mb-DDAB-PAA	TCE	10–100	2	0.997	14
Mb-DDAB-PVS	TCA	10–100	4	0.999	22
Mb-DDAB-PSS	BHC	1.3–50	1	0.997	23
Mb-DDAB-PSS	TCE	125–1220	60	0.996	23

Generally, HRP in films showed catalytic reactivity similar to that of Mb and Hb. For example [36], in clay films cast on PG electrodes, all the three proteins incorporated could catalyze reduction of O_2, H_2O_2, and TCA. However, HRP-clay films demonstrated different catalytic properties than the others. Table 4 lists the catalytic efficiency for different substrates (O_2, H_2O_2, and TCA) with the three protein-clay films. For oxygen and hydrogen peroxide, HRP-clay films seem to be more active than Mb- and Hb-clay films, while for trichloroacetic acid, HRP-clay films are much less active than the other films in its catalytic reductions.

Table 4 Catalytic efficiency (I_c/I_d) of different substrates with protein-clay films [36].

Film	O_2[a]	H_2O_2[b]	TCA[c]
Mb-clay	3.0	3.0	2.0
Hb-clay	3.1	3.6	2.0
HRP-clay	5.2	3.8	1.1

[a]0.2 V s^{-1}, 30 mL air passed in 9 mL solution.
[b]0.2 V s^{-1}, 0.22 mM H_2O_2.
[c]0.2 V s^{-1}, 50 mM TCA.

The mechanism of catalytic reduction of these organochlorides with protein films might be expressed as Scheme 1 [37]. Here, we take protein heme Fe(III)/Fe(II) redox couple as an example.

$$\text{HemeFe(III)} + e^- \rightleftarrows \text{HemeFe(II)} \qquad \text{at electrode}$$

$$\text{HemeFe(II)} + \text{RCl} \rightarrow \text{HemeFe(III)} + R^\bullet + Cl^- \qquad \text{rds}$$

$$\text{HemeFe(II)} + R^\bullet + H^+ \rightarrow \text{HemeFe(III)} + \text{RH} \qquad \text{fast}$$

The overall reaction would be:

$$\text{RCl} + H^+ + 2e^- \rightarrow \text{RH} + Cl^-$$

Scheme 1

CONCLUSIONS

Various kinds of films modified on electrode surface may provide a favorable microenvironment for redox proteins to transfer electron directly with electrodes. Only very small amounts of protein are needed to make the films. The protein films show excellent stability in aqueous solutions. When being used as the foundation of biosensors or bioreactors for monitoring or destroying organohalide pollutants, the protein films demonstrate good catalytic properties. They make great lowering of overpotential required by reduction of the substrates, indicating a large decrease in activation energy. The protein films also show good selectivity. Proteins or enzymes have some selectivity toward different substrates. Meanwhile, different films may show different permselectivity to substrates. Thus, direct electrochemistry of protein films not only can be used as a model for mechanism study of electron transfer between proteins or enzymes in real living system, but also can be employed as the basis of fabricating biosensor or bioreactor, and may have significance in practical application.

As the extension of our above works, other types of films such as layer-by-layer [38,39] films, are also used to incorporate proteins. Studies of direct electrochemistry of proteins in these new types of films are underway in our laboratory.

ACKNOWLEDGMENT

The support of the National Natural Science Foundation of China is acknowledged.

REFERENCES

1. M. F. Chaplin and C. Bucke. *Enzyme Technology*, Cambridge University Press, Cambridge (1990).
2. F. A. Armstrong and G. S. Wilson. *Electrochim. Acta* **45**, 2623 (2000).
3. A. Heller. *Acc. Chem. Res.* **23**, 128 (1990).
4. F. A. Armstrong. In *Bioinorganic Chemistry, Structure and Bonding 72*, pp. 137–236, Springer-Verlag, Berlin (1990).
5. M. J. Eddowes and H. A. O. Hill. *J. Chem. Soc. Chem. Commun.* 771 (1977).
6. J. F. Rusling. *Acc. Chem. Res.* **31**, 363 (1998).
7. J. F. Rusling and A.-E. F. Nassar. *J. Am. Chem. Soc.* **115**, 11891 (1993).
8. F. A. Armstrong, J. Hirst, H. A. Heering. *Chem. Soc. Rev*. **26**, 169 (1997).
9. P. Bianco and J. Haladjian. *J. Electroanal. Chem*. **367**, 79 (1994).
10. P. Bianco, A. Taye, J. Haladjian. *J. Electroanal. Chem*. **377**, 299 (1994).
11. Z. Zhang, A.-E. F. Nassar, Z. Lu, J. B. Schenkman, J. F. Rusling. *J. Chem. Soc., Faraday Trans*. **93**, 1769 (1997).
12. T. Ferri, A. Poscia, R. Santucci. *Bioelectrochem. Bioenerg*. **45**, 221 (1998).
13. J. Yang, N. Hu. *Bioelectrochem. Bioenerg.* **48**, 117 (1999).
14. Y. Hu, N. Hu, Y. Zeng. *Talanta* **50**, 1183 (2000).
15. R. W. Murray. In *Electroanalytical Chemistry*, Vol. 13, A. J. Bard (Ed.), pp. 191–368, Marcel Dekker, New York (1984).
16. X. Chen, N. Hu, Y. Zeng, J. F. Rusling, J. Yang. *Langmuir* **15**, 7022 (1999).
17. A. M. Bond. *Modern Polarographic Methods in Analytical Chemistry*, pp. 29–30, Marcel Dekker, New York (1980).
18. J. G. Osteryoung and J. J. O'Dea. In *Electroanalytical Chemistry*, Vol. 14, A. J. Bard (Ed.), pp. 209–325, Marcel Dekker, New York (1986).
19. J. J. O'Dea and J. G. Osteryoung. *Anal. Chem.* **65**, 3090 (1993).
20. Z. Zhang and J. F. Rusling. *Biophys. Chem.* **63**, 133 (1997).

21. A.-E. F. Nassar, Z. Zhang, N. Hu, J. F. Rusling, T. F. Kumosinski. *J. Phys. Chem. B* **101**, 2224 (1997).
22. Y. Hu, N. Hu, Y. Zeng. *Microchem. J.* **65**, 147 (2000).
23. H. Ma and N. Hu. *Anal. Lett.* **34**, 339 (2001).
24. L. Wang and N. Hu. *J. Colloid Interface Sci.* **236**, 166 (2001).
25. N. Hu, Z. Li, H. Ma. *Gaodeng Xuexiao Huaxue Xuebao (Chem. J. Chinese Univ.)* **22**, 450 (2001).
26. N. Hu and J. F. Rusling. *Langmuir* **13**, 4119 (1997).
27. H. Sun, H. Ma, N. Hu. *Bioelectrochem. Bioenerg.* **49**, 1 (1999).
28. J. Yang, N. Hu, J. F. Rusling. *J. Electroanal. Chem.* **463**, 53 (1999).
29. H. Sun, N. Hu, H, Ma. *Electroanalysis* **12**, 1064 (2000).
30. R. Huang and N. Hu. *Bioelectrochemistry* **54**, 75 (2001).
31. P. George and G. I. H. Hanania. *Biochem. J.* **55**, 236 (1953).
32. T. F. Kumosinski and J. J. Unruh. In *Molecular Modeling*, ACS Symposium Series 576, T. F. Kumosinski and M. N. Liebman (Eds.), pp. 71–98, Washington, DC (1994).
33. G. Cevc and D. Marsh. *Phospholipid Bilayers*, Wiley, New York (1987).
34. A-E. F. Nassar, Z. Zhang, V. Chynwat, H. A. Frank, J. F. Rusling, K. Suga. *J. Phys. Chem. B* **99**, 11013 (1995).
35. C. P. Andrienx, C. Blocman, J. M. Dumas-Bouchiat, F. M'Halla, J. M. Saveant. *J. Electroanal. Chem.* **113**, 19 (1980).
36. Y. Zhou, N. Hu, Y. Zeng, J. F. Rusling. *Langmuir* **18**, 211 (2002).
37. A.-E. F. Nassar, J. M. Bobbitt, J. O. Stuart, J. F. Rusling. *J. Am. Chem. Soc*. **117**, 10986 (1995).
38. H. Ma, N. Hu, J. F. Rusling. *Langmuir* **16**, 4969 (2000).
39. L. Wang and N. Hu. *Bioelectrochemistry* **53**, 205 (2001).